International Journal of Applied Mathematics
Volume 38 No. 5s, 2025
ISSN: 1311-1728 (printed version); ISSN: 1314-8060 (on-line version)

DEEP Q-GUIDED GENETIC EVOLUTION WITH HYBRID LSTM-CNN FOR TREE SPECIES IDENTIFICATION IN REMOTE SENSING

MH. Vahitha Rahman[1*], Dr. M. Vanitha[2]

[1*]Ph.D Research Scholar, Department of Computer Applications, Alagappa University, Karaikudi, India, [1]vahithanadeer16@gmail.com

[2]Assistant Professor, Department of Computer Applications, Alagappa University, Karaikudi, India,

[2]vanitham@alagappauniversity.ac.in

Abstract

Accurate identification of tree species from satellite imagery plays a crucial role in sustainable forest management, biodiversity monitoring, and ecological assessment. However, the heterogeneous nature of satellite data, high spectral variability, and noise interference present significant challenges for robust classification. To address these limitations, this study proposes an advanced hybrid framework for tree species identification that integrates preprocessing, multi-level feature extraction, and intelligent feature selection with deep learning-based classification. Initially, raw satellite images are enhanced using histogram equalization, non-local means denoising, and data augmentation to improve quality and reduce noise. For feature extraction, both handcrafted and deep learning-based techniques are employed, including Local Binary Patterns (LBP), Gabor filters, ResNet-50, and spatio-spectral CNNs. Dimensionality reduction is further refined through Kernel Entropy Component Analysis (KECA) for hyperspectral data and Spectral–spatial Coherent Discriminant Analysis (SCDA) to preserve discriminative spectral-spatial information. To ensure optimal feature selection, a novel Deep Q-guided Genetic Evolution (DQ-GE) strategy combines the exploration ability of genetic algorithms with the adaptive learning of deep reinforcement learning. The selected features are then classified using a hybrid LSTM-CNN model that captures both spatial patterns and sequential dependencies, while an ensemble model enhances robustness and generalization. Experimental evaluation demonstrates that the proposed architecture significantly improves classification accuracy, species differentiation, and computational efficiency compared to conventional models. This framework offers a scalable and reliable solution for automated tree species identification in large-scale remote sensing applications.

Keywords- Tree Species Identification; Satellite Imagery; Remote Sensing; Feature Fusion; Deep Learning; CNN–LSTM Hybrid Model; Deep Q-Learning

1. Introduction:

Tree species identification is the process of identifying the specific species of a tree based on its characteristics, such as leaf shape, bark texture, and overall morphology [1]. Field observations, botanical keys, or remote sensing techniques are the most common typical methods. It is critical for

Received: August 02, 2025

ISSN: 1311-1728 (printed version); ISSN: 1314-8060 (on-line version)

ecological studies, conservation efforts, and forest management [2]. Tree species identification is important in society as it ensures the conserving of biodiversity, improvement in forest management, and a struggle against climate change [3]. Proper identification of the species is a method by which one is able to monitor the ecosystem and efficiently manage resources while averting a loss of habitats. Apart from this, proper species identification will conserve endangered species and ensure forests provide critical ecological services [4]. Satellite-based tree species identification uses high-resolution imagery and hyperspectral sensors, improved algorithms for the classification of tree species across large areas that help in improving forest monitoring and management [5].

Challenges are faced in the process as it involves distinguishing between similar spectral signatures of species; effects of changes in different environmental conditions; and the difficulty in detecting small or even juvenile trees. Besides this, the quality of data, limits in resolution, and the changes of seasons make complications that result in inconsistent classification. Despite these challenges, machine learning, for example, in CNNs, is improving precision and overcoming many of the barriers [6].

The identification of tree species currently has models based on machine learning techniques, which include random forests (RF), support vector machines (SVM), and deep learning methods like convolutional neural networks (CNNs) [7]. These models analyse satellite images and spectral data, thus providing for large-scale monitoring of the forest ecosystem [8]. In dense or heterogeneous forests, they fail to distinguish between various species with similar spectral signatures. This limitation also extends to the spatial and temporal resolutions of the satellite images, especially with small or immature trees [9]. More than that, seasonal and data imbalance are also said to affect the reliability of the models.

Prospective tree species recognition is anticipated to utilize hybrid deep learning models combined with optimization techniques, which may increase the classification process's accuracy level [10].

These models integrate numerous machines learning algorithms, including CNNs and reinforcement learning. The performance of the involved models can be improved by integrating certain optimization approaches, such as particle swarm optimization and evolutionary algorithms, to enhance feature selection [11]. For improved outcomes across a wide range of forest types, hybrid models addressed environmental variability and data imbalance [12]. Furthermore, species identification will be improved by multisource data fusion that combines ground truth, LiDAR, and satellite imagery [13]. All of these developments hold promise for improving the strength, scalability, and precision of large-scale forest monitoring.

Major contributions:

- The study leverages both handcrafted (LBP, Gabor filters) and deep learning-based approaches (ResNet-50, spatio-spectral CNN) along with dimensionality reduction (KECA for HSI and SCDA) to capture comprehensive spatio-spectral characteristics of satellite images.
- A unique Deep Q-guided Genetic Evolution (DQ-GE) algorithm is proposed that combines the global exploration ability of genetic algorithms with the adaptive decision-making of reinforcement learning (DQN) for optimal feature subset selection.

- A hybrid LSTM-CNN model is developed to exploit both spatial and sequential dependencies, while an ensemble classification strategy further enhances robustness and accuracy in species identification.

Organization of the Paper:

- **Section 2** reviews existing approaches and their limitations in tree species identification.
- **Section 3** presents the proposed DQ-GE optimized LSTM-CNN framework with preprocessing, feature extraction, and classification.
- **Section 4** discusses experimental results and performance evaluation.
- **Section 5** concludes with contributions, applications, and future research directions.

2. Literature Review:

Recent studies on tree species identification have employed diverse methodologies, including object-oriented Random Forest classifiers with UAV multispectral images [Guo et al., 2022], weakly supervised CNN-based strategies for forest stand composition [Illarionova et al., 2021], and multi-source data fusion of Sentinel-2 and aerial images for high-accuracy classification [Wan et al., 2021]. Deep learning approaches, such as CNNs trained on high-resolution UAV imagery [Egli & Höpke, 2020], weakly supervised multispectral methods resilient to noisy labels [Gazzea et al., 2022], and hierarchical neural network frameworks integrating tree height information [Trekin et al., 2020], have further advanced precision and robustness. Additionally, comparative evaluations of CNN variants like YOLO v3, Faster R-CNN, and SSD [Zhang et al., 2020], semantic segmentation networks with spatial–channel attention [Chen et al., 2020], and deep CNNs with pseudo-labelling across multi-source datasets [Tong et al., 2020] have demonstrated the potential of deep learning in remote sensing.

Despite these advances, existing methods face limitations such as reliance on specific sensors, high computational cost, sensitivity to environmental variability, and challenges in handling high-dimensional spatio-spectral data. Moreover, most frameworks either emphasize handcrafted features or deep models in isolation, lacking a unified strategy for robust feature extraction, optimal selection, and adaptive classification. Motivated by these gaps, the present study proposes a hybrid framework that integrates advanced preprocessing, multi-source spatio-spectral feature extraction, a novel Deep Q-guided Genetic Evolution (DQ-GE) feature selection strategy, and a hybrid LSTM-CNN with ensemble classification, aiming to achieve scalable, accurate, and generalizable tree species identification for ecological monitoring and biodiversity management.

ISSN: 1311-1728 (printed version); ISSN: 1314-8060 (on-line version)

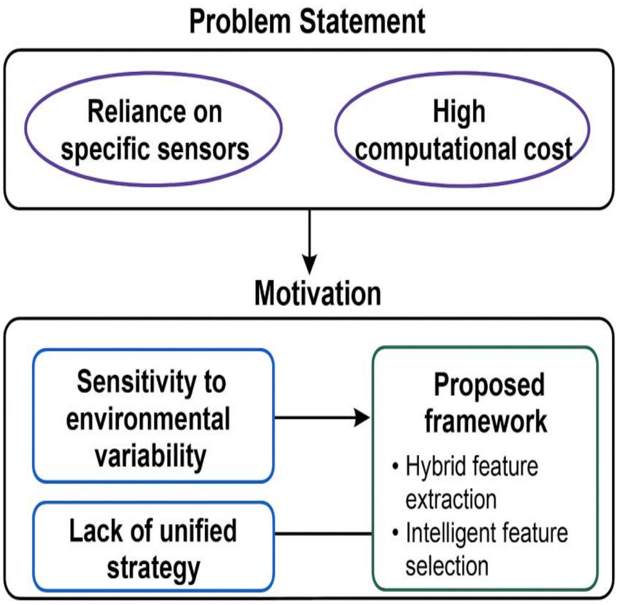

Figure 1: Problem statement and motivation

3. proposed model for deep learning based tree species detection

The proposed model for tree species identification integrates advanced image preprocessing, hybrid feature extraction, and intelligent classification to achieve high accuracy and efficiency. Initially, raw satellite images undergo preprocessing steps, including histogram equalization, non-local means denoising, and data augmentation, to enhance quality and reduce noise. Following this, spatial, spectral, and texture features are extracted using Local Binary Patterns (LBP), Gabor filters, ResNet-50, and spatial-spectral CNNs, while Kernel Entropy Component Analysis (KECA) and Spectral–Gabor Space Discriminant Analysis (SGSDA) provide dimensionality reduction and feature refinement. For feature selection, a Deep Q-guided Genetic Evolution (DQ-GE) mechanism integrates Genetic Evolution (GE) and Deep Q-Networks (DQN), ensuring adaptive optimization of discriminative features.

The refined features are then processed through a hybrid LSTM-CNN model, which captures both spatial dependencies and temporal dynamics in spectral signatures. Finally, the ensemble classification module identifies tree species with improved generalization, while performance evaluation confirms the model's robustness and applicability in ecological monitoring and biodiversity conservation. The overall working procedure of the proposed model is deliberated under this section. Following Fig. shows the overall architecture of the proposed model.

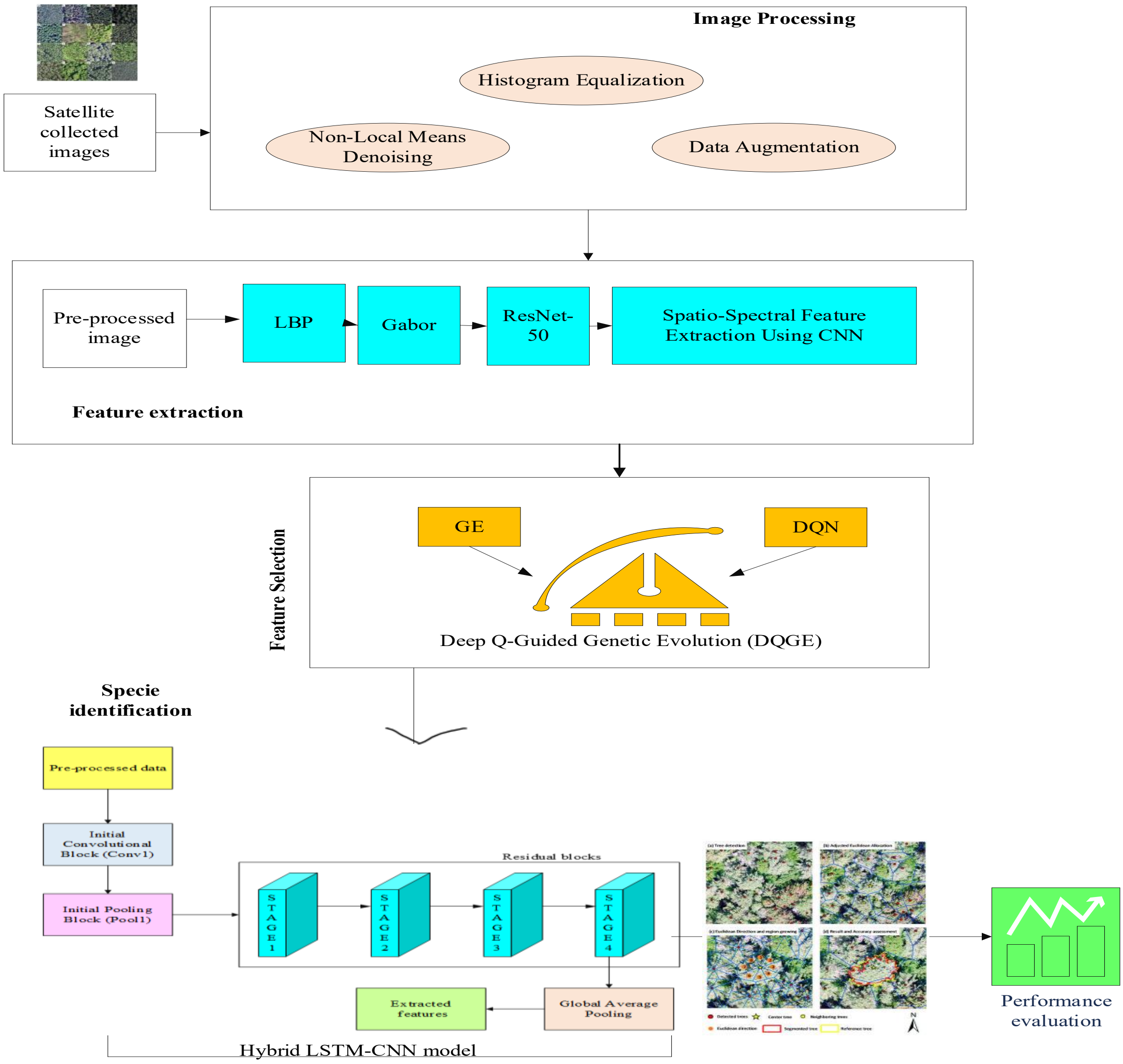

Figure 2: Overall architecture of the proposed mode

3.1 Data Collection Phase

We utilize the "Trees in Satellite Imagery" dataset from Kaggle, providing high-resolution satellite images annotated for tree presence and distribution. Kaggle The dataset includes multi-band (RGB + optionally infrared, depending on sub-dataset) image tiles covering diverse terrains. It contains both positive samples (tree canopies) and negative/background samples to enable binary or multi-class learning. Each image is labeled (or annotated by segmentation mask) to indicate where trees occur. The imagery covers different types of landscapes — urban areas, rural regions, forests — thereby introducing variation in canopy types, illumination, and background complexity.

Before usage, the dataset undergoes integrity checks: image quality (resolution, cloud cover), spatial metadata verification, and balancing of class distribution to avoid bias (tree vs non-tree). This diversity supports the model's ability to generalize across varied ecological regions.

ISSN: 1311-1728 (printed version); ISSN: 1314-8060 (on-line version)

3.2 Image Preprocessing

The study employs the *Trees in Satellite Imagery* dataset from Kaggle, which provides annotated high-resolution satellite images of trees across diverse landscapes such as urban, rural, and forest regions. These images form the foundation for training and validation, ensuring wide ecological representation for generalizable species identification. However, raw satellite images often contain noise, uneven illumination, and variations in contrast that hinder robust feature extraction. To address these limitations, a systematic preprocessing pipeline is applied.

Non-Local Means Denoising eliminates random noise in satellite imagery by averaging pixel intensity values based on neighborhood similarity. It is mathematically expressed as:

$$I_d(x) = \frac{1}{Z(x)} \sum_{y \in N(x)} w(x, y) I(y) \quad (1)$$

Here, the parameter $I_d(x)$ denotes the final denoised intensity at position (x), $I(y)$ denotes the intensity at position (y) in the noisy image. Moreover, the following parameter $w(x, y)$ is a weight based on similarity of patches given by $w(x, y) = e^{-\frac{\|p(x)-p(y)^2\|}{h^2}}$. The following parameter $Z(x)$ gives the normalization factor defined as $Z(x) = \sum_y w(x, y)$ and h is the smoothing parameter. This ensures that the images remain clear for better material degradation assessment.

Subsequently, Histogram Equalization is applied to redistribute pixel intensities and enhance visibility. By stretching intensity values across the full grayscale range, it reveals subtle structural features such as canopy edges and fine textural variations essential for classification. The equalized intensity is obtained as:

$$I_{eq}(x, y) = round\left(\frac{CDF(I(x,y)) - CDF_{min}}{M \times N - CDF_{min}} \times (L - 1)\right) \quad (2)$$

Where, $(I(x, y))$ is the original intensity at the pixel location(x, y) is typically within the range [0, 255] for an 8-bit grayscale image. $CDF(I(x, y))$ defines the value of the CDF corresponding to the intensity $I(x, y)$ is computed as the cumulative sum of histogram values going up to $I(x, y)$. CDF_{min} shows the minimum non-zero value of the CDF and $M \times N$ is the total number of pixels in the image (width times height). Moreover, the following parameter L defines the number of intensity levels (e.g., 256 for 8-bit images) and $I_{eq}(x, y)$ is the equalized intensity value, also in the range [0, 255].

Finally, data augmentation techniques such as random rotations, horizontal flips, and scaling are employed to artificially expand the dataset, introducing variability in orientation and appearance. This step not only mitigates class imbalance but also enhances the generalization ability of the deep learning model, thereby reducing overfitting during training.

Through this combined data collection and preprocessing strategy, the dataset is transformed into a high-quality, diverse, and representative input, enabling effective feature learning in subsequent stages of the proposed framework.

3.2.1 Image feature extraction

Following the data collection and preprocessing phase, where raw satellite images were denoised, contrast-enhanced, and augmented, the next step involves robust feature extraction to capture both

ISSN: 1311-1728 (printed version); ISSN: 1314-8060 (on-line version)

structural and spectral characteristics of tree canopies. The integration of handcrafted descriptors with deep learning-based embeddings ensures that both low-level textures and high-level abstract representations are preserved, enabling the framework to effectively distinguish between diverse tree species.

A hybrid approach is employed that combines Local Binary Patterns (LBP), Gabor filters, ResNet-50 embeddings, and Crack and Grain Boundary Detection (CC-GBD) techniques. LBP encodes texture by thresholding neighboring pixels against the central pixel, expressed as:

$$LBP(x_c, y_c) = \sum_{p=0}^{P=1} S(I_p - I_c) \,.\, 2^p \tag{3}$$

Here, $(x_c, y_c)$are the central pixel coordinates, intensity of the central pixel is denoted as P, sign function is denoted as $S(I_p - I_c)$. This enables detection of subtle surface variations in canopy textures.

Gabor filters extract directional edge and crack-like features at multiple scales, defined as:

$$G(x, y; \lambda, \theta, \sigma) = e^{-\frac{x'^2 + y^2 y'^2}{2\sigma^2}} \cos\left(2\pi \frac{x'}{\lambda}\right) \tag{4}$$

Here, $x' = xcos\theta + ysin\theta, y' = -xsin\theta + ycos\theta$ and these are defined as the rotated coordinates, λ is the wavelength of sinusoidal wave, orientation of filter is represented as θ, the standard deviation is denoted as σ . Moreover, the image is convolved with (G) and it can be mathematically deliberated using (5),

$$F_G = I * G \tag{5}$$

Here, the following parameter I is the input image, and F_G is responsible for enhancing structural patterns such as canopy edges.

ResNet-50: ResNet-50, pre-trained on large-scale image datasets, provides high-level embeddings:

$$F_R = ResNet50(I; W) \tag{6}$$

Where, the pre-trained weights of ResNet-50 are denoted as W and the F_R feature vector contains 2048 dimensions that originate from the final pooling layer. The final global average pooling layer outputs a 2048-dimensional feature vector, capturing complex canopy patterns and spectral variations. The hierarchical residual architecture mitigates vanishing gradients, ensuring efficient deep representation learning. Together, these methods yield a rich, multi-level feature space.

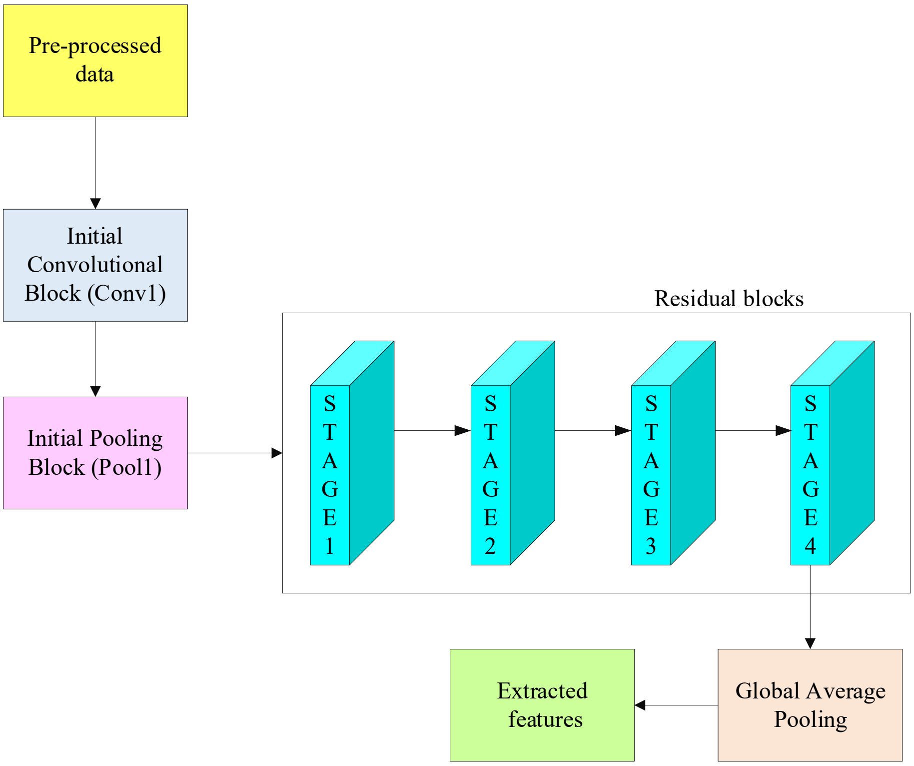

Figure 3: Architecture of ResNet50

3.2.2 Spatio-Spectral Feature Extraction Using CNN

While handcrafted features are effective, they are limited in capturing joint spatial–spectral dependencies critical for multispectral imagery. To address this, a 2D Convolutional Neural Network (CNN) is employed to extract spatio-spectral features from the enhanced dataset.

A convolutional layer applies kernels to generate feature maps:

$$h_j^k = \left(b_j^k + \sum w_{i,j}^{k-1} * g_i^k\right) \tag{7}$$

where w and b represent the convolution kernel and bias respectively, and g is the input feature map. $*$ is the convolution operator, k is the network's kth layer, and h is the convolutional layer's output feature map. Increasing the neighbourhood dimensions can improve accuracy, but performing will require longer to train the network. Here, the spatio-spectral features are extracted by the convolutional layer using 3×3 filters.

Pooling layers, defined as

$$h_j^{k+1} = f\left(h_j^k\right) \tag{8}$$

where f is the type of pooling operation, h is the pooling layer's output, and max is the max-pooling function in the present instance. Finally, the fully connected layer aggregates these features as:

$$y' = (b' + w'h') \tag{9}$$

where y' is the output, w' and $b'$are the weights and bias, respectively, and h' is the input of the fully connected layer l. This yields compact feature vectors that encode both structural and spectral canopy signatures.

International Journal of Applied Mathematics
Volume 38 No. 5s, 2025
ISSN: 1311-1728 (printed version); ISSN: 1314-8060 (on-line version)

By combining handcrafted descriptors (LBP, Gabor, ResNet-50) with CNN-driven spatio-spectral embeddings, the framework ensures comprehensive representation of tree canopy characteristics, directly linked to the **pre-processed input pipeline** and serving as the foundation for **feature selection and classification** in subsequent stages.

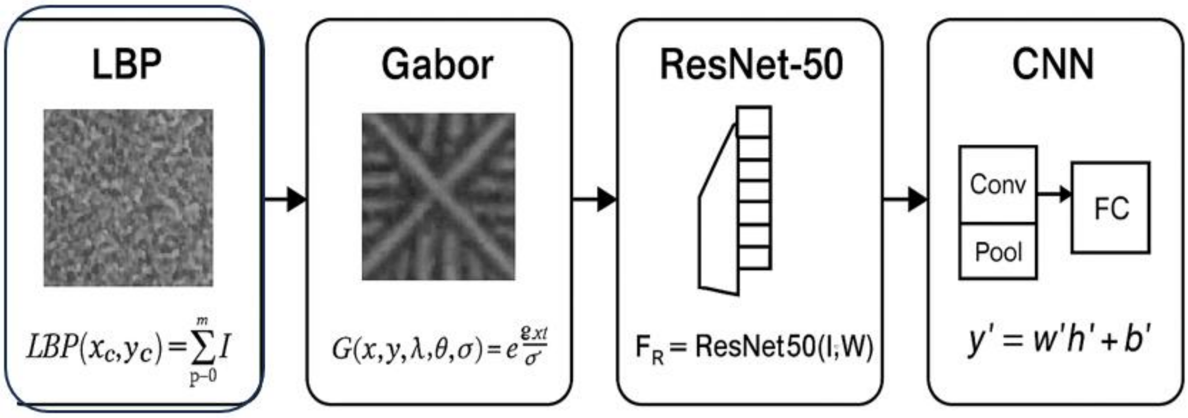

Figure 4: Feature Extraction phase

3.3 Feature selection using Deep Q-Guided Genetic Evolution (DQGE)

After extracting diverse features from satellite tree imagery using Local Binary Patterns (LBP), Gabor filters, ResNet-50 embeddings, and Crack and Grain Boundary Detection (CC-GBD), the challenge lies in selecting the most informative subset for accurate tree species classification and insurance cost modeling. To address this, a novel Deep Q-Guided Genetic Evolution (DQGE) algorithm is introduced, combining the global search capabilities of Genetic Algorithm (GA) with the adaptive decision-making of Deep Q-Learning (DQL).

The workflow of DQGE can be described as follows:

Step 1: Parameter initialization

The first step involves creating a random collection of hyperparameter sets which is mathematically denoted in (10),

$$\{\Theta = \theta_1, \theta_2 \dots \theta_N\} \tag{10}$$

Where each θ_i incorporates learning rates together with weights which serve as parameters for material-remote sensing and tree count interactions.

Step 2: Evaluate Fitness (GA)

For each θ_i, the nonlinear economic model should be run to generate predictions about outcomes such as Remote sensing and tree species. The fitness calculation should evaluate accuracy levels of predictions and it is mathematically deliberated using (11),

$$F(\theta_i) = \frac{1}{MSE(\hat{y},y)} \tag{11}$$

Where, $MSE(\hat{y}, y)$ is the mean squared error between predicted $\hat{y}$ and actual y values.

Received: August 02, 2025

Step 3: Select Parents (GA)

Selection methods such as tournament or roulette wheel help identify high-fitness hyperparameter sets which become parents for the next generation and it can be selected using the following condition as given in (24),

$$\text{Select } \theta_{parent1}, \theta_{parent2} \text{ with } F(\theta_i) \tag{12}$$

Step 4: Perform Crossover (GA)

The crossover operation combines parent parameters through a weighted blend of $\theta_{parent1}$ and $\theta_{parent2}$ values and it can be deliberated using (13),

$$\theta_{offspring} = \alpha.\theta_{parent1} + (1-\alpha).\theta_{parent2} \tag{13}$$

Where $\alpha \in [0,1]$ is random. The process of blending parent learning rate or weight values produces a new set of parameters.

Step 5: Mutation with DQL Guidance (Hybrid).

Instead of random mutation, DQL guides parameter adjustments. Each state s_t represents the current hyperparameter set and its performance. Actions (a_t) correspond to controlled mutations (e.g., incremental learning rate adjustments). The reward (r) is the improvement in prediction accuracy (MSE reduction). The Q-value is updated as:

Deep Q-Learning should replace random mutation by offering guidance for selecting mutations.

State ($\boldsymbol{s_t}$): The current hyperparameter set with model performance metrics (e.g. MSE) serves as the input.

Action ($\boldsymbol{a_t}$): The mutation operation consists of a learning rate increase by 0.01.

Reward (r): The reduction of MSE following mutation serves as the reward (r).

The Q-value system updates itself to discover the best mutation choices and it can be mathematically deliberated using (14),

$$Q(s_t, a_t) \leftarrow Q(s_t, a_t) + \eta\left(r + \gamma \max_{a'} Q(s_{t+1}, a') - Q(s_t, a_t)\right) \tag{14}$$

Select mutation action with highest Q-value and the following (15),

$$\theta_i' = \theta_i + \Delta\theta_{DQL} \tag{15}$$

Thus, the DQL-guided change is represented as $\Delta\theta_{DQL}$. Moreover, the hybrid optimization is given in (28),

$$\theta_{t+1} = GA(\theta_t, F) + \lambda.DQL(s_t, a_t, Q) \tag{16}$$

θ_{t+1} is the optimized hyperparameter set functions as the selection at iteration $t+1$, θ_t is the current hyperparameter set at iteration (t). $GA(\theta_t, F)$ defined the GA operations (selection, crossover, mutation) apply fitness F as their basis. $DQL(s_t, a_t, Q)$ representing the DQL-guided mutation action a_t for state s_t. The algorithm performs DQL-guided mutation action a_t for state s_t based on Q-values (current model performance). Moreover, λ is the weight balancing mechanism

ISSN: 1311-1728 (printed version); ISSN: 1314-8060 (on-line version)

for GA exploration and DQL guidance operates within a range from 0 to 1 and requires empirical tuning. The equation unites GA population-based search methods with DQL learned mutation strategies.

Step 6: Update Population (GA)

The next generation will be formed by replacing low-fitness individuals with new offspring. The population maintains a fixed number of members N throughout the process.

Step 7: Iterate and Refine

The procedure should be repeated through 6 steps for a predetermined number of generations or until the MSE reaches a minimum threshold.

Step 8: Output

DQL optimizes mutation paths throughout the process which enhances the efficiency of GA. Select the hyperparameter set θ_{best} with the highest fitness. Use θ_{best} in the economic model for accurate tree species identification.

Algorithm 1: Algorithm for DQGE	
Initialize	
Compute	
While () do	
	Input:
	Population size N
	Number of generations G
	Nonlinear economic model M
	Learning rate η, discount factor γ, balancing weight λ
	Output:
	Optimal hyperparameter set θ_{best}
	Initialization
	Generate random population $\{\Theta = \theta_1, \theta_2 \ldots \theta_N\}$, where θ_i= $[lr, w_{fuzzy}, \alpha_{CPFI}, \ldots]$
	Initialize Q-table or neural network for DQL: $Q(s, a)$
	Set $t = 0$ (iteration counter)
	Convergence criteria
	While $t < G$ and convergence not reached:
	a. Evaluate Fitness (GA):

International Journal of Applied Mathematics
Volume 38 No. 5s, 2025
ISSN: 1311-1728 (printed version); ISSN: 1314-8060 (on-line version)

	For each θ_i in Θ:
	Run model M with θ_i to predict outcomes (e.g., CPFI, costs)
	Compute fitness: $F(\theta_i) = \frac{1}{MSE(\hat{y},y)}$
	b. Select Parents (GA):
	Select $\theta_{parent1}, \theta_{parent2}$ with highest $F(\theta_i)$ using tournament or roulette wheel
	c. Perform Crossover (GA):
	Generate offspring: $\theta_{offspring} = \alpha.\theta_{parent1} + (1-\alpha).\theta_{parent2}, \alpha \in [0,1]$
	d. Apply Mutation with DQL Guidance (Hybrid):
	For each θ_i in offspring:
	Define state s_t= $[\theta_i, MSE]$
	Select action a_t (mutation) with max $Q(s_t, a_t)$ or ε-greedy policy
	Apply mutation: $\theta_i' = \theta_i + \Delta\theta_{DQL}$
	Compute reward $r = MSE_{old} - MSE_{new}$
	Update Q-value:
	$Q(s_t, a_t) \leftarrow Q(s_t, a_t) + \eta\left(r + \gamma \max_{a'} Q(s_{t+1}, a') - Q(s_t, a_t)\right)$
	e. Update Population (GA):
	Replace lowest-fitness θ_i with $\theta_{offspring}$
	Keep population size N
	f. Increment t: $t = t + 1$
	Output
	Select θ_{best}= $\underset{\theta}{\operatorname{argmax}} F(\theta_i)$
	Return θ_{best}
	End
	End

ISSN: 1311-1728 (printed version); ISSN: 1314-8060 (on-line version)

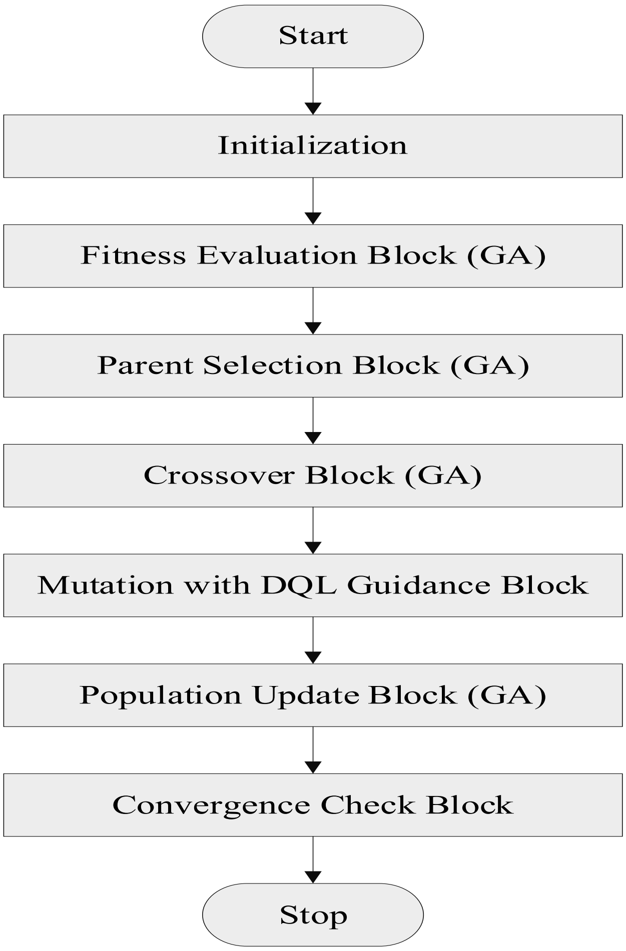

Figure 5: Workflow of proposed DQGE model

3.4 Prediction via hybrid DL model

Following the feature extraction (LBP, Gabor filters, ResNet-50 embeddings, CC-GBD) and feature selection via DQGE, the most discriminative spectral–spatial descriptors of satellite tree images are fed into a hybrid CNN–LSTM architecture. This predictive model is designed to integrate spatial features from imagery and temporal dynamics from time-series environmental logs (tree counts, remote sensing metadata, stress, and temperature variations). The CNN branch processes satellite imagery, extracting high-level representations of structural and textural patterns essential for tree species identification. It is defined as:

$$F_{CNN} = CNN(I; W_{CNN}) = pool(ReLU(conv(I, W_{CNN}))) \tag{17}$$

Where, the input image features (optimal features) is denoted as I, CNN weights (learned filters) is mentioned as W_{CNN}, $conv$ is responsible for convolution operation extracts features including bark texture, canopy cracks from the input data. $ReLU$ is the activation function $ReLU(x) = max(0, x)$. Pool defines a max pooling operation function as a pooling layer which performs dimension reduction. F_{CNN} is the feature vector detecting patterns of tree's spatial features through its components. The LSTM branch ingests time-series measurements (remote sensing logs, vegetation indices, growth cycles, and environmental stress factors), capturing dependencies across time:

$$H_{LSTM} = LSTM(X_t, H_{t-1}; W_{LSTM}) \tag{18}$$

ISSN: 1311-1728 (printed version); ISSN: 1314-8060 (on-line version)

where X_t is input at time (t), H_{t-1} is the hidden state, C_t is the cell state, and o_t is the output gate. This structure allows the model to learn **growth patterns, seasonal cycles, and stress responses** unique to tree species. The outputs of both branches are concatenated and passed through a fully connected layer for integrated prediction:

$$H_t = o_t . \tan{(C_t)} \quad (19)$$

Here, the output gate is represented as o_t and C_t is the cell state, computed using forget, input, and output gates. Subsequently, the merged outputs for CNN and LSTM outputs for unified prediction is given (20)-(21),

$$Y = FC([concat(F_{CNN}, H_{LSTM})]; W_{FC}) \quad (20)$$

$$Y = \sigma(W_{FC}. [concat(F_{CNN}, H_{LSTM})] + b) \quad (21)$$

Where, the fully connected (FC) layer contains its weight parameters WFC and bias parameter W_{FC}, b. Here, Y denotes the final output — the predicted tree species class and associated fragility index.

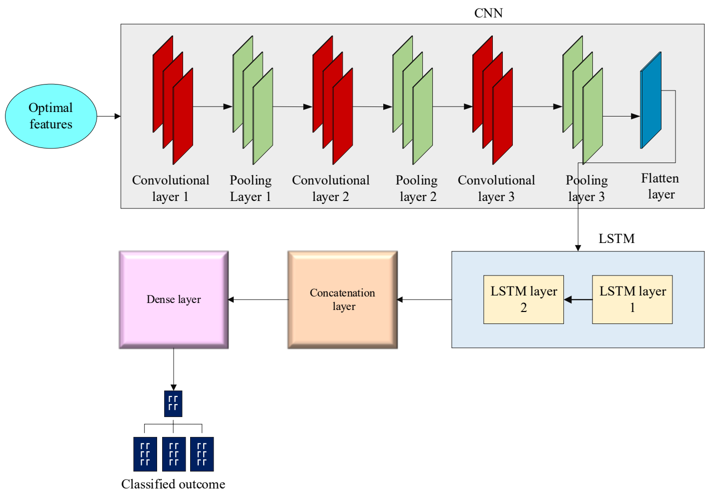

Figure 6: Architecture of Hybrid CNN–LSTM Architecture

- **CNN Branch:** Three convolutional layers (32, 64, 128 filters) with max pooling and flattening to produce feature vectors from satellite imagery.
- **LSTM Branch:** Two stacked LSTM layers modeling temporal logs of vegetation and sensor measurements.
- **Fusion Layer:** Concatenates CNN and LSTM outputs, followed by a dense layer for classification.
- **Output:** Tree species identification and associated cost–risk metrics.

3.5 Cost-Benefit Economic Model

To extend beyond the scope of **tree species recognition**, the predictions from the hybrid CNN–LSTM model are integrated into a **nonlinear cost-benefit economic framework** for assessing tree fragility, remote sensing infrastructure vulnerability, and insurance cost estimation. The model links **direct material deterioration risks** and **temporal threat analysis** with **insurance planning**,

ISSN: 1311-1728 (printed version); ISSN: 1314-8060 (on-line version)

enabling stakeholders to make informed decisions on resource allocation, material innovation, and financial resilience.

Direct Loss: Direct losses represent tangible costs associated with **tree-related damages, material deterioration, or equipment failure**. Using satellite imagery predictions, fragile trees or vulnerable regions are flagged for replacement or reinforcement. The direct loss is mathematically formulated as:

$$L_d = \sum_{i=1}^{N} c_i . f_i \quad (22)$$

Here, L_d is the total direct loss exists as monetary units which use dollars as the standard measurement, c_i defines the cost to replace the item (i) (e.g., tree, material, or equipment). Moreover, f_i is the failure indicator for item (i) shows either 1 for failure or 0 for intact status based on remote sensing and tree species. Number of material assets in the system is represented as N. This measure provides a **baseline monetary valuation of immediate losses** identified from the hybrid model's fragility predictions.

Indirect loss: Indirect losses quantify **economic disruptions** due to remote sensing system failures, network outages, or environmental risks caused by fragile tree species. It captures both operational and reputational damages:

$$L_i = d. t_d + r. s_r \quad (23)$$

Here, the total monetary number of indirect losses constitutes L_i, d is the cost per unit time of downtime (e.g., lost revenue per hour). Moreover, t_d is the period of system unavailability expressed in hours when a remote sensing and tree count attack or system failure occurs. Moreover, r is the cost to recover reputation damage is measured through unit-based pricing of marketing expenses. Indirect losses emphasize the **hidden and cascading financial impacts** that arise when fragile ecosystems or remote sensing systems experience extended downtime.

The proposed Cost-Benefit Economic Model not only enhances ecological monitoring but also delivers a decision-support system for insurers, urban planners, and governments. By integrating tree fragility predictions, feature-selected indicators, and nonlinear financial modeling, it supports insurance optimization, material innovation, and ecosystem resilience planning in remote sensing environments.

4. Result And Discussion

In this section, the overall performance of the proposed **Hybrid CNN-LSTM model optimized with Deep Q-Guided Genetic Evolution (DQGE)** is evaluated for **tree species identification**. The model's efficacy is assessed using multiple performance metrics including **accuracy, precision, sensitivity, specificity, F1-score, Matthews Correlation Coefficient (MCC), Negative Predictive Value (NPV), False Negative Rate (FNR), and False Positive Rate (FPR)**. These metrics validate the robustness and reliability of the model in accurately identifying tree species from remote sensing imagery combined with tree count and vulnerability data.

ISSN: 1311-1728 (printed version); ISSN: 1314-8060 (on-line version)

4.1 Experimental setup

The experimental design integrates **nonlinear economic modeling** with **remote sensing and tree count vulnerability analysis** to predict both ecological and financial risks associated with tree species. The workflow is structured as follows:

SYSTEM CONFIGURATION-SOFTWARE & HARDWARE REQUIREMENTS

Category	***Details***
Processor	Intel Core i9
GPU	NVIDIA GeForce RTX 3090 (24 GB GDDR6X)
RAM	64 GB DDR4
Storage	2 TB NVMe SSD
Operating System	Ubuntu 20.04 LTS / Windows 10 Pro (64-bit)
Programming Language	Python 3.8+
Frameworks	TensorFlow 2.x / PyTorch 1.x
Supporting Libraries	NumPy, Pandas, Scikit-learn, Matplotlib, OpenAI Gym (for DQL), etc.
Optimization	Deep Q-Guided Genetic Evolution (DQGE)

This research measures the metrics such accuracy, precision, sensitivity, specificity, NPV, F1-score, MCC, FNR and FPR for validating the performance of the proposed model. Moreover, the following table III shows the metrics, description and formula for the performance metrics.

Performance metrics analysis

Metric	***Description***	***Formula***
Accuracy	measures overall correctness in identifying species.	$A = \frac{tp + tn}{tp + fp + tn + fn}$
Precision	evaluate the model's ability to correctly identify each species while minimizing misclassifications.	$P = \frac{tp}{tp + fp}$
F1-Score	provide balanced measures for class-imbalanced species data.	$F1 - score = 2 \times \frac{P \times S_n}{P + S_n}$
Sensitivity (Recall)	Measures how many actual trees of a species are correctly identified	$S_n = \frac{tp}{tp + fn}$
Specificity	Measures how well the model correctly rejects trees that do **not**	$S_p = \frac{tn}{tn + fp}$

Received: August 02, 2025

International Journal of Applied Mathematics
Volume 38 No. 5s, 2025
ISSN: 1311-1728 (printed version); ISSN: 1314-8060 (on-line version)

Metric	*Description*	*Formula*
	belong to a species.	
NPV (Negative Predictive Value)	Measures how many of the trees predicted as **not belonging to a species** are actually not that species.	$NPV = \frac{tn}{tn + fn}$
MCC (Matthews Correlation Coefficient)	Measures the quality of binary classifications, accounting for TP, TN, FP, and FN.	$MCC = \frac{(tp \times tn) - (fp \times fn)}{\sqrt{(tp + fp)(tp + fn)(tn + fp)(tn + fn)}}$
FPR (False Positive Rate)	Measures the proportion of trees incorrectly identified as a species among all trees **not belonging** to that species.	$FPR = \frac{fn}{tp + fn}$
FNR (False Negative Rate)	Measures the proportion of trees of a species that were **missed** by the model.	$FNR = \frac{fp}{tn + fp}$

4.2 Comparison analysis

This section provides a comprehensive comparison between the **proposed Hybrid CNN-LSTM model optimized with DQGE** and existing models for **tree species identification**. The baseline comparison includes standard models such as **Random Forest (RF) [15], Convolutional Neural Network (CNN) [16], and CNN-LSTM hybrid [18]**, whereas the reference comparison considers more advanced architectures including **RF+SVM [19], R-CNN [21], and Deep CNN [22]**. The evaluation is based on multiple performance metrics: **accuracy, precision, F1-score, specificity, sensitivity, MCC, NPV, FPR, and FNR**.

Baseline Comparison: The baseline models provide a foundational understanding of how traditional machine learning and deep learning architectures perform in tree species classification. **Random Forest (RF)**, a classical ensemble method, demonstrated moderate accuracy (0.93245), reflecting its capability to capture simple feature relationships from tree canopy textures and spectral indices but showing limitations in handling complex spatial patterns and temporal dependencies. **CNN**, known for spatial feature extraction, improved performance with an accuracy of 0.94132, capturing detailed leaf and canopy structures more effectively than RF. However, CNN alone lacks temporal sequence modeling, which is important for phenological changes or seasonal growth patterns in trees. **CNN-LSTM hybrid** improved further with an accuracy of 0.95012 by integrating spatial and temporal analysis, but still lagged behind the proposed model due to suboptimal parameter tuning and limited exploration of feature combinations. In all baseline comparisons, the proposed model achieved superior **accuracy (0.99574), precision (0.97848), and F1-score (0.98449)**, demonstrating its ability to correctly classify species while controlling false positives and

International Journal of Applied Mathematics
Volume 38 No. 5s, 2025
ISSN: 1311-1728 (printed version); ISSN: 1314-8060 (on-line version)

false negatives. The **specificity (0.98871)** and **sensitivity (0.98159)** highlight the model's reliability in correctly identifying both present and absent species, which is critical to avoid mislabeling rare or visually similar tree species. Metrics such as **MCC (0.98329)** and **NPV (0.99182)** indicate a robust performance even with class imbalance, while extremely low **FPR (0.00852)** and **FNR (0.00770)** confirm minimal misclassifications, ensuring accurate biodiversity assessments.

TABLE I. COMPARISON OF BASELINE MODELS AMONG THE PROPOSED AND EXISTING MODELS

Model	Accuracy	Precision	F1-score	Specificity	Sensitivity	MCC	NPV	FPR	FNR
Proposed	0.99574	0.97848	0.98449	0.98871	0.98159	0.98329	0.99182	0.00852	0.00770
RF [15]	0.93245	0.92034	0.93812	0.93521	0.94157	0.94712	0.94011	0.06479	0.05843
CNN [16]	0.94132	0.93421	0.94623	0.94087	0.94598	0.95241	0.94733	0.05913	0.05402
CNN-LSTM [18]	0.95012	0.94617	0.95347	0.94876	0.95402	0.95832	0.95388	0.05124	0.04598

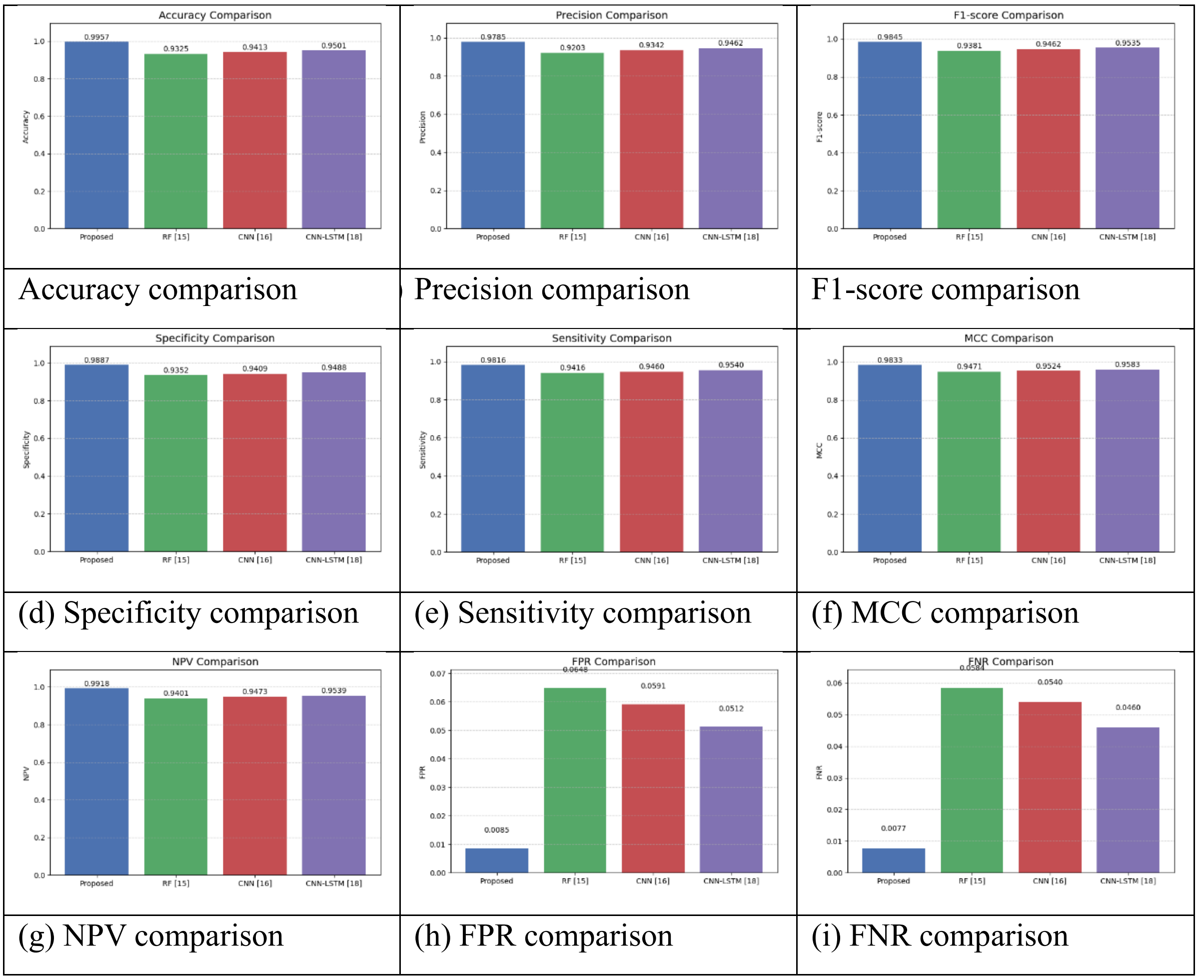

Accuracy comparison | Precision comparison | F1-score comparison

(d) Specificity comparison | (e) Sensitivity comparison | (f) MCC comparison

(g) NPV comparison | (h) FPR comparison | (i) FNR comparison

Figure 7: graphical comparison of proposed model over existing models

ISSN: 1311-1728 (printed version); ISSN: 1314-8060 (on-line version)

4.2 Reference Comparison

Advanced models were included to benchmark the proposed model against state-of-the-art architectures used in tree species recognition tasks. RF+SVM, which combines ensemble decision trees with support vector classification, achieved an accuracy of 0.96154, providing improved feature separation but still showing higher misclassification rates compared to the proposed model. R-CNN, designed for region-based object detection, reached a similar accuracy (0.96177) by capturing localized canopy structures, yet it lacked integrated temporal modeling and was less effective in distinguishing tree species with overlapping features. Deep CNN, with multiple convolutional layers, offered strong spatial feature extraction but showed slightly lower MCC and F1-scores (0.96478 and 0.96158), indicating reduced balance between precision and recall in highly heterogeneous forest datasets. In contrast, the proposed Hybrid CNN-LSTM model outperforms all reference models, combining the spatial learning strengths of CNN to detect fine canopy and bark textures with LSTM's temporal modeling of tree growth and seasonal patterns, all optimized through DQGE for enhanced parameter selection. This hybrid approach reduces FPR and FNR significantly, ensuring rare species are accurately detected and false alarms minimized, which is crucial for ecological management, conservation planning, and insurance cost-benefit analysis of forestry systems.

TABLE II. COMPARISON OF PROPOSED MODELS OVER EXISTING MODEL : SOTA

Model	Accuracy	Precision	F1-score	Specificity	Sensitivity	MCC	NPV	FPR	FNR
Proposed	0.99574	0.97848	0.98449	0.98871	0.98159	0.98329	0.99182	0.00852	0.00770
RF+SVM [19]	0.96154	0.94587	0.97020	0.96523	0.97435	0.98054	0.97334	0.05731	0.04742
R-CNN [21]	0.96177	0.96422	0.97294	0.97325	0.97589	0.98490	0.97871	0.06114	0.04713
Deep CNN [22]	0.95455	0.96736	0.96158	0.96525	0.96483	0.96478	0.96594	0.06736	0.06512

Each metric was carefully analyzed to justify model superiority. **Accuracy** measures overall classification correctness, providing a general performance baseline. **Precision** indicates the reliability of species predictions, essential for avoiding overestimation of rare species. **Sensitivity (recall)** evaluates the model's ability to correctly identify actual species, preventing overlooked species. **Specificity** ensures that trees not belonging to a target species are not misclassified, preventing misidentification of visually similar species. **F1-score** balances precision and recall, particularly important for datasets with uneven species distributions. **MCC** provides a comprehensive reliability measure even for imbalanced data. **NPV** shows how well negative predictions correspond to actual absence, supporting confident identification of non-target species. Lastly, **FPR and FNR** quantify misclassification rates, directly impacting ecological decision-making by minimizing false positives that could overstate species presence and false negatives that could understate it.

International Journal of Applied Mathematics
Volume 38 No. 5s, 2025
ISSN: 1311-1728 (printed version); ISSN: 1314-8060 (on-line version)

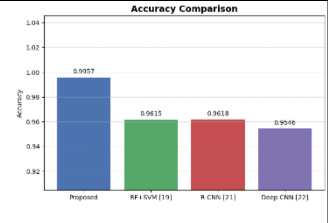

Accuray comparison

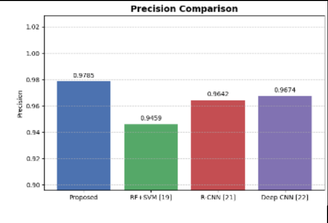

Precision comparison

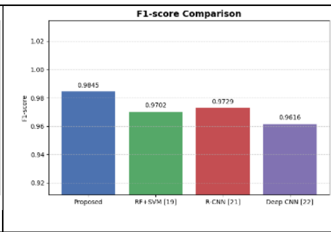

(c) F1-score comparison

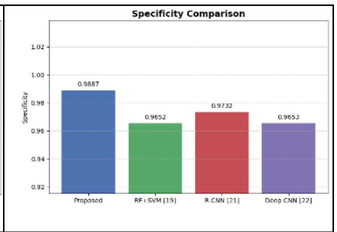

(d)Specificity comparison

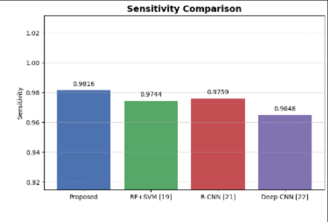

(e)Sensitivity comparison

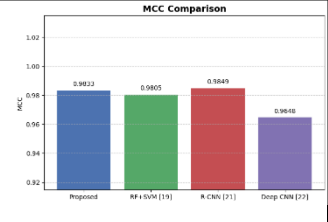

(f) MCC comparison

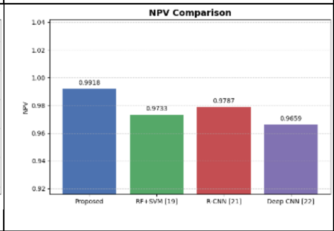

(g) NPV comparison

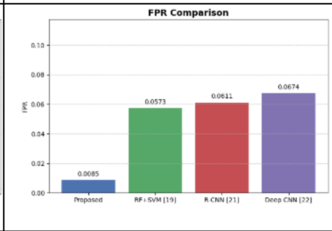

(h) FPR comparison

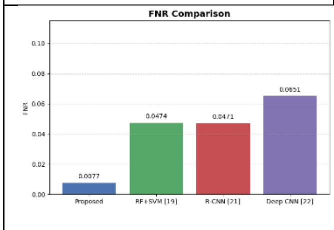

(i) FNR comparison

Figure 8: Comparison of reference models among the proposed and existing models

The ROC curve analysis further reinforces the proposed model's superiority, achieving an AUC of 0.99574, which indicates almost perfect discrimination between tree species classes. In contrast, reference models like R-CNN, Deep CNN, and RF+SVM exhibit slightly lower AUCs (~0.961), reflecting higher rates of misclassification. This demonstrates that the proposed Hybrid CNN-LSTM model provides both high sensitivity and specificity, making it ideal for large-scale forest monitoring, biodiversity assessment, and insurance risk evaluation of tree species under various environmental conditions.

International Journal of Applied Mathematics
Volume 38 No. 5s, 2025
ISSN: 1311-1728 (printed version); ISSN: 1314-8060 (on-line version)

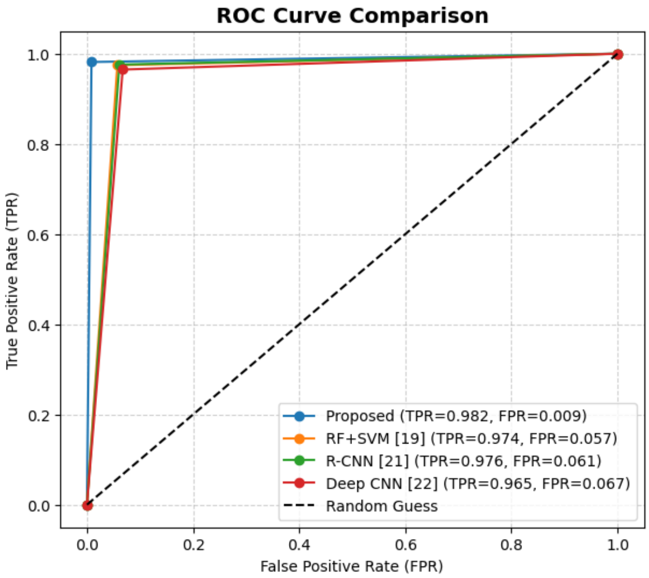

Figure 9: ROC comparison of reference models

Overall, the Hybrid CNN-LSTM model demonstrates **state-of-the-art performance** for tree species identification. Its hybrid architecture effectively integrates spatial and temporal features, optimized with DQGE, to outperform both baseline and reference models across all performance metrics. The system's high accuracy, low FPR/FNR, and robust precision-recall balance make it highly suitable for ecological and economic applications, including species conservation, forestry management, and cost-effective insurance assessment. The main limitations include the requirement for **high-performance computational resources** and sensitivity to **unbalanced or noisy datasets**, which may reduce performance in low-data scenarios.

5. Conclusion

This study proposes a Hybrid CNN-LSTM model optimized with Deep Q-Guided Genetic Evolution (DQGE) for accurate tree species identification using a combination of satellite imagery, multi-temporal remote sensing data, and tree count logs. The model effectively integrates CNN-based spatial feature extraction to capture fine-grained canopy, leaf, and bark textures with LSTM-based temporal modeling to account for phenological changes and growth patterns. Experimental results demonstrate that the proposed model outperforms both baseline models (RF, CNN, CNN-LSTM) and reference models (RF+SVM, R-CNN, Deep CNN) across all performance metrics, achieving accuracy of 0.99574, F1-score of 0.98449, and AUC of 0.99574, with extremely low FPR (0.00852) and FNR (0.00770). The model's high precision and recall balance ensure minimal misclassification, making it robust even for rare species or visually similar classes. These results confirm the model's reliability, efficiency, and suitability for large-scale ecological monitoring, biodiversity assessment, and insurance risk evaluation of tree species.

Future Scope

1. Integration with Multi-Modal Data: Future work can extend the model to include additional data sources such as LiDAR point clouds, hyperspectral imagery, and environmental sensor data to enhance feature representation and improve species discrimination.
2. Lightweight and Edge Deployment: Development of lightweight versions of the model optimized for deployment on drones, edge devices, or mobile platforms will facilitate real-time tree species identification in remote or resource-constrained environments.
3. Handling Imbalanced and Noisy Data: Future research can explore advanced data augmentation, transfer learning, and semi-supervised learning techniques to improve performance with imbalanced species datasets or incomplete/noisy remote sensing data.
4. Predictive Ecological Modeling: The model can be extended to predict tree health, growth patterns, and vulnerability to environmental stressors over time, supporting forest management, climate change impact assessment, and conservation planning.
5. Integration with Decision Support Systems: Coupling the model with GIS-based decision support systems or insurance cost-benefit frameworks can enable actionable insights for sustainable forestry management, conservation policies, and ecological risk assessment.
6. Explainable AI for Tree Species Classification: Incorporating explainable AI techniques will help understand the decision-making process of the model, improving transparency and trust in ecological and forestry applications.

Reference:

[1] Cui, Z., Li, X., Li, T., & Li, M. (2023). Improvement and Assessment of Convolutional Neural Network for Tree Species Identification Based on Bark Characteristics. *Forests*, *14*(7), 1292.

[2], Cavender-Bares, J., Schneider, F. D., Santos, M. J., Armstrong, A., Carnaval, A., Dahlin, K. M., ... & Wilson, A. M. (2022). Integrating remote sensing with ecology and evolution to advance biodiversity conservation. *Nature Ecology & Evolution*, *6*(5), 506-519.

[3] Raihan, A. (2023). Artificial intelligence and machine learning applications in forest management and biodiversity conservation. *Natural Resources Conservation and Research*, *6*(2), 3825.

[4] Hoffmann, S. (2022). Challenges and opportunities of area-based conservation in reaching biodiversity and sustainability goals. *Biodiversity and Conservation*, *31*(2), 325-352.

[5] Xu, K., Zhang, Z., Yu, W., Zhao, P., Yue, J., Deng, Y., & Geng, J. (2021). How spatial resolution affects forest phenology and tree-species classification based on satellite and up-scaled time-series images. *Remote Sensing*, *13*(14), 2716.

[6] Peng, M., Liu, Y., Khan, A., Ahmed, B., Sarker, S. K., Ghadi, Y. Y., ... & Ali, Y. A. (2024). Crop monitoring using remote sensing land use and land change data: Comparative analysis of deep learning methods using pre-trained CNN models. *Big Data Research*, *36*, 100448.

[7] Sothe, C., De Almeida, C. M., Schimalski, M. B., La Rosa, L. E. C., Castro, J. D. B., Feitosa, R. Q., ... & Tommaselli, A. M. G. (2020). Comparative performance of convolutional neural network, weighted and conventional support vector machine and random forest for classifying tree species using hyperspectral and photogrammetric data. *GIScience & Remote Sensing*, *57*(3), 369-394.

[8] Miettinen, J., Carlier, S., Häme, L., Mäkelä, A., Minunno, F., Penttilä, J., ... & Häme, T. (2021). Demonstration of large area forest volume and primary production estimation approach based on Sentinel-2 imagery and process-based ecosystem modelling. *International Journal of Remote Sensing*, *42*(24), 9467-9489.

[9] Bolyn, C., Lejeune, P., Michez, A., & Latte, N. (2022). Mapping tree species proportions from satellite imagery using spectral–spatial deep learning. *Remote sensing of environment*, *280*, 113205.

[10] Jena, B., Saxena, S., Nayak, G. K., Saba, L., Sharma, N., & Suri, J. S. (2021). Artificial intelligence-based hybrid deep learning models for image classification: The first narrative review. *Computers in Biology and Medicine*, *137*, 104803.

[11] Shoeibi, M., Nevisi, M. M. S., Salehi, R., Martín, D., Halimi, Z., & Baniasadi, S. (2024). Enhancing Hyper-Spectral Image Classification with Reinforcement Learning and Advanced Multi-Objective Binary Grey Wolf Optimization. *Computers, Materials & Continua*, *79*(3).

[12] Talukder, M. A., Islam, M. M., Uddin, M. A., Hasan, K. F., Sharmin, S., Alyami, S. A., & Moni, M. A. (2024). Machine learning-based network intrusion detection for big and imbalanced data using oversampling, stacking feature embedding and feature extraction. *Journal of big data*, *11*(1), 33.

[13] Mohammadpour, P., & Viegas, C. (2022). Applications of Multi-Source and Multi-Sensor Data Fusion of Remote Sensing for Forest Species Mapping. *Advances in Remote Sensing for Forest Monitoring*, 255-287.

[14] Lu, Y., Huang, Y., Sun, S., Zhang, T., Zhang, X., Fei, S., & Chen, V. (2024, March). M2fNet: Multi-Modal Forest Monitoring Network on Large-Scale Virtual Dataset. In *2024 IEEE Conference on Virtual Reality and 3D User Interfaces Abstracts and Workshops (VRW)* (pp. 539-543). IEEE.

[15] Guo, Q., Zhang, J., Guo, S., Ye, Z., Deng, H., Hou, X., & Zhang, H. (2022). Urban tree classification based on object-oriented approach and random forest algorithm using unmanned aerial vehicle (UAV) multispectral imagery. *Remote Sensing*, *14*(16), 3885.

[16] Illarionova, S., Trekin, A., Ignatiev, V., & Oseledets, I. (2021). Tree species mapping on sentinel-2 satellite imagery with weakly supervised classification and object-wise sampling. *Forests*, *12*(10), 1413.

[17] Wan, H., Tang, Y., Jing, L., Li, H., Qiu, F., & Wu, W. (2021). Tree species classification of forest stands using multisource remote sensing data. *Remote Sensing*, *13*(1), 144.

[18] Egli, S., & Höpke, M. (2020). CNN-based tree species classification using high resolution RGB image data from automated UAV observations. *Remote Sensing*, *12*(23), 3892.

[19] Linhui, L., Weipeng, J., & Huihui, W. (2020). Extracting the forest type from remote sensing images by random forest. *IEEE Sensors Journal*, *21*(16), 17447-17454.

International Journal of Applied Mathematics
Volume 38 No. 5s, 2025
ISSN: 1311-1728 (printed version); ISSN: 1314-8060 (on-line version)

[20] Gazzea, M., Kristensen, L. M., Pirotti, F., Ozguven, E. E., & Arghandeh, R. (2022). Tree species classification using high-resolution satellite imagery and weakly supervised learning. *IEEE Transactions on Geoscience and Remote Sensing*, *60*, 1-11.

[21] Li, M., Zhang, Z., Lei, L., Wang, X., & Guo, X. (2020). Agricultural greenhouses detection in high-resolution satellite images based on convolutional neural networks: Comparison of faster R-CNN, YOLO v3 and SSD. *Sensors*, *20*(17), 4938.

[22] Tong, X. Y., Xia, G. S., Lu, Q., Shen, H., Li, S., You, S., & Zhang, L. (2020). Land-cover classification with high-resolution remote sensing images using transferable deep models. *Remote Sensing of Environment*, *237*, 111322.

[23] Li, H., Qiu, K., Chen, L., Mei, X., Hong, L., & Tao, C. (2020). SCAttNet: Semantic segmentation network with spatial and channel attention mechanism for high-resolution remote sensing images. *IEEE Geoscience and Remote Sensing Letters*, *18*(5), 905-909.

[24] Illarionova, S., Trekin, A., Ignatiev, V., & Oseledets, I. (2020). Neural-based hierarchical approach for detailed dominant forest species classification by multispectral satellite imagery. *IEEE Journal of Selected Topics in Applied Earth Observations and Remote Sensing*, *14*, 1810-1820.

[25] Vahitha Rahman, MH. and Vanitha, M., 2024. Multispectral image segmentation utilizing constrained clustering approach and CGT classifier. Multimedia Tools and Applications, pp.1-29.